Biosensors and Bioelectronics 53 (2014) 440–446

Contents lists available at ScienceDirect

Biosensors and Bioelectronics

journal homepage: www.elsevier.com/locate/bios

Covalent fabrication of methyl parathion hydrolase on gold nanoparticles modified carbon substrates for designing a methyl parathion biosensor

Guozhen Liu *, Wenqi Guo, Zhang Yin

Key Laboratory of Pesticide and Chemical Biology of Ministry of Education, College of Chemistry, Central China Normal University, Wuhan 430079, PR China

ARTICLE INFO

Article history:
Received 28 July 2013
Received in revised form
10 October 2013
Accepted 11 October 2013
Available online 24 October 2013

Keywords:
AuNP
Au–C bonding
Methyl parathion hydrolase
Aryldiazonium salts
Methyl parathion

ABSTRACT

A biosensor based on AuNP modified GC electrodes has been developed for direct detection of methyl parathion. AuNP can be introduced to mixed monolayers of aryldiazonium salt modified GC electrodes by Au–C bonding through aryldiazonium salt chemistry, which provides a stable interface showing efficient electron transfer between biomolecules and electrodes. PEG molecules were introduced to the interface to resist non-specific protein adsorption. AuNP surfaces were further modified with 4-carboxyphenyl followed by covalent immobilization of methyl parathion hydrolase (MPH), a specific biocatalytic enzyme to methyl parathion. Exposure of this interface to methyl parathion resulted in a change in amperometric signal due to the MPH catalytic hydrolysis of methyl parathion producing electroactive compound 4-nitrophenol. This biosensor shows high selectivity, specificity, reproducibility and stability, and is functional for the detection of methyl parathion in real samples. The linear range for detection of methyl parathion is 0.2–100 ppb with a detection limit of 0.07 ppb in 0.1 M phosphate buffer at pH 7.0.

1. Introduction

Organophosphate pesticides such as paraoxon and parathion derivatives are highly toxic agricultural chemicals that are still used extensively worldwide to control a wide range of insect species. Accidental exposure of humans and domestic animals to such insecticides results in a potentially lethal cholinergic poisoning (Giordano and Collins, 2007; Mercey et al., 2012). It is therefore essential to develop a method for rapid, specific, and sensitive monitoring the levels of these insecticides in environmental samples. Traditional techniques such as chromatography are generally performed for detection organophosphate pesticides with good sensitivity and accuracy (Leandro et al., 2007). However, they are very expensive, time-consuming, and not suitable for in field measurement. Attractively, biological approaches afford rapid, specific, and sensitive detection as well as compatibility with miniaturized and portable devices (Gao et al., 2012; Oliveiraa et al., 2012; Sharmaa et al., 2012). The acetylcholinesterase (AChE) is one of the popular enzymes used for biosensors for detection of organophosphate pesticides due to the strong inhibition and wide substrate specificity. However, the inhibition reactions generally require long incubation time for sufficient sensitivity and long regeneration time of the inhibited enzyme necessary for reusing the sensors (Gaberlein et al., 2000). With the unique biocatalytic activity of organophosphous hydrolase (OPH) to a range of organophosphates, OPH based biosensors take steps further for detection of organophosphorus compounds (Chough et al., 2002; Gong et al., 2009; Sacks et al., 2000; Zhao et al., 2013). Especially methyl parathion hydrolase (MPH) has demonstrated high specificity to methyl parathion (Du et al., 2010). Zhang's group has prepared a MPH based nanocomposite biosensor for highly sensitive and selective determination of methyl parathion with a detection limit of 0.3 ng mL^{-1} (Chen et al., 2011). However, it is desirable to improve the stability of this biosensor.

Designing an effective biorecognition interface is critical to the performance of a biosensor, such as stability, reproducibility, specificity, and sensitivity. The modification of immunosensing interface with nanomaterials such as carbon nanotubes and nanoparticles to achieve enhanced properties has received considerable attention in electroanalytical chemistry (Katz et al., 2004). Compared to carbon nanotubes, metal nanoparticles, especially gold nanoparticles (AuNP), as the more homogeneous nanomaterial have been extensively studied because of their attractive physicochemical characteristics, such as high surface-to-volume ratio, good biocompatibility, and being able to facilitate electron transfer between biomolecules and electrode (Zhao et al., 2005). The majority of AuNP modified interfaces are based on the affinity between thiols and gold to form S–Au bond or the affinity between amines and gold to form NH–Au bond, which offers a simple, fast and versatile approach for preparing nanoelectrode

* Corresponding author. Tel.: +86 27 6786 7535.
E-mail address: gzliu@mail.ccnu.edu.cn (G. Liu).

0956-5663/$ - see front matter © 2013 Elsevier B.V. All rights reserved.
http://dx.doi.org/10.1016/j.bios.2013.10.025

arrays with low background capacitance. Electrochemically reductive adsorption of aryldiazonium salts in acetonitrile or aqueous solutions with pH below 2 is a popular method of surface modification (Gooding, 2008). AuNP also can be covalently modified on the electrodes by Au–C bonding through diazonium salt chemistry, which is firstly reported by Liu et al. (2011, 2012). AuNP tethered on interfaces by Au–C bonding is much more stable than that by forming S–Au and NH–Au bonds, which presents an interesting issue for sensing applications. More recently GutiéRrez-SáNchez et al. (2012) reported a stable nanostructured enzymatic electrode based on covalent attachment of AuNPs to porous graphite electrodes by Au–C bonding.

Here we aim to develop a sensing interface based on covalent anchoring AuNP on carbon substrates followed by covalent immobilization of MPH for detection of methyl parathion. The electrodes were firstly derivatised with mixed monolayers of 4-aminophenyl/PEG followed by the assembly of AuNP by Au–C binding, which provided an interface for efficient electron transfer between the substrate and the target analyte, while effectively resisting the nonspecific adsorption of protein. For covalent coupling of biological molecules, 4-carboxyphenyl species were introduced to the surface of AuNP followed by attachment of MPH. The MPH catalytic hydrolysis of methyl parathion produces dimethyl phosphate and the electroactive 4-nitrophenol (Dong et al., 2005). Based on the redox reaction of *p*-nitrophenol, the fabricated biosensor can be used to detect methyl parathion electrochemically.

2. Materials and methods

2.1. Chemicals and instruments

Sodium nitrite, potassium ferricyanide, potassium chloride, hydrochloric acid, acetonitrile (CH_3CN, HPLC grade), tetrabutylammonium tetrafluoroborate (NBu_4BF_4), *N*-hydroxysuccinimide (NHS), 1-ethyl-3-(3-dimethyl aminopropyl) carbodiimide hydrochloride (EDC), hydrogen tetrachloroaurate (III), and tri-sodium citrate (99% purity) were purchased from Sigma-Aldrich (Shenshi Huagong, Wuhan). Culture media and supplements were from Gibco (HaoranBio, Shanghai). Culture plastic wares were from Bibby Sterilin Ltd. (Stone, UK). The aryldiazonium cations for 4-nitrophenyl, 4-carboxyphenyl, and PEG were synthesized as reported previously (Liu et al., 2005; Liu and Gooding, 2006). AuNPs were synthesized using a 1 mM solution of $HAuCl_4$ in Milli-*Q* water that was boiled prior to adding tri-sodium citrate with constant stirring. A colour change started to occur 10 s after the addition of citrate solution according to the method of Frens (1973). All reagents were used as received, and aqueous solutions were prepared with DI water. Phosphate buffer solution used in this work contained 0.05 M KCl and 0.05 M K_2HPO_4/KH_2PO_4 adjusted to pH 7.0 with NaOH or HCl solution.

2.2. Preparation of the purified MPH

The expression and purification of MPH was carried out according to the method described in the literature (Sun et al., 2004). A single colony of Pseudomonas sp. WBC-3 (Sanyi Chemicals, Wuhan) was cultured for 48 h at 303 K with shaking in 20 mL Luria-Bertani medium containing 100 mg mL^{-1} ampicillin. The cells were harvested by centrifugation at 8000 rpm for 10 min at 277 K to reach the OD of 0.6. Following harvesting, the cell pellets were resuspended in buffer A (10 mM KH_2PO_4 pH 7.0) and then disrupted by sonicating 200 times for 4 s periods at 6 s intervals. The cellular residue was removed by centrifugation of lysates at 15,000 rpm for 30 min at 277 K and the supernatant was stored at 277 K for purification. All the purification steps were performed at 289 K. The clear supernatant was loaded onto a 16 mL CM-Sepharose Fast Flow Column from Pharmacia (Sanyi Chemicals, Wuhan) previously equilibrated with buffer A. The protein was then eluted using a linear gradient of NaCl from 0 to 0.56 M in buffer A at a low rate of 1 mL min^{-1}. The fractions containing the highest MPH activity were collected and concentrated by centrifugation on a 5 K ultrafiltration membrane. Further purification was achieved by gel-filtration chromatography on Superdex G75 from Pharmacia pre-equilibrated with buffer B (20 mM Tris–HCl pH 7.6 and 80 mM NaCl). The target protein MPH was eluted from the column with buffer B and the peak fractions were combined and concentrated to 40 ± 50 mg mL^{-1} using a 5 K ultrafiltration membrane.

2.3. Preparation of sensing interface for detection of methyl parathion

Scheme 1 shows the process for preparation of sensing interface for detection of methyl parathion. Prior to modification, GC electrodes were polished successively with 1.0, 0.3, and 0.05 μm alumina slurries (Buehler, USA) on microcloth pads (Buehler). The electrodes were thoroughly rinsed and sonicated in Milli-*Q* water for 1 min between polishing steps. Before modification, electrodes were dried with a stream of argon. The derivatization of the clean GC electrode with mixed monolayers of 4-nitrophenyl/PEG (GC-Ph-NO_2/PEG) was carried out in an acetonitrile solution of 1 mM mixed diazonium salt and 0.1 M NBu_4BF_4 using cyclic voltammetry (CV) with a scan rate of 100 mV s^{-1} for two cycles between +1.0 and −1.0 V versus Ag/AgCl. The diazonium salt solution was deaerated with argon for at least 10 min prior to derivatization of the electrode. The obtained 4-nitrophenyl groups on GC electrodes could be reduced electrochemically to 4-aminophenyl groups in a protic solution (90:10 v/v H_2O–EtOH + 0.1 M KCl). Then the terminal amine groups can be converted to diazonium groups by incubating GC-Ph-NH_2/PEG modified interface in a basic solution (phosphate buffer, pH = 10) containing 10 mM $NaBH_4$ for overnight. Subsequently the electrode was rinsed with copious amounts of acetonitrile and then Milli-*Q* water and dried under a stream of argon prior to the next step. AuNPs were covalently coupled to the cleaned electrode by electrochemistry at fixed potential of −0.4 V versus Ag/AgCl in AuNP solution for 240 s following by cycling the AuNP modified electrodes in an acetonitrile solution of 1 mM 4-carboxylphenyl diazonium salt and 0.1 M NBu_4BF_4 for two cycles with a scan rate of 100 mV s^{-1} between +0.5 V and −0.6 V versus Ag/AgCl. The carboxylic acid groups on the modified surface was activated by EDC/NHS, and then the activated GC electrodes were incubated in 0.1 M phosphate buffer (pH 7.0) containing 1 mg mL^{-1} MPH for 12 h at 4 °C to achieve the MPH modified sensing surface.

2.4. Analysis of spiked real samples

Each 100 g of soil sample and green tea sample were collected and sprayed with 0.5 mL 200 ppb methyl parathion. Samples were kept in air at room temperature for overnight to imitate the field condition. Afterwards, Samples were soaked in 10 mL 0.1 M phosphate buffer solution pH7.0 with stirring for 1 h. The top liquid part was collected for analysis. Four water samples were directly spiked with methyl parathion to get the final concentration of 20 ppb before analysis.

2.5. Electrochemistry measurements and surface analysis

All electrochemical experiments were conducted using GaosUnion EC510 potentiostats. GC electrodes were 3 mm disks

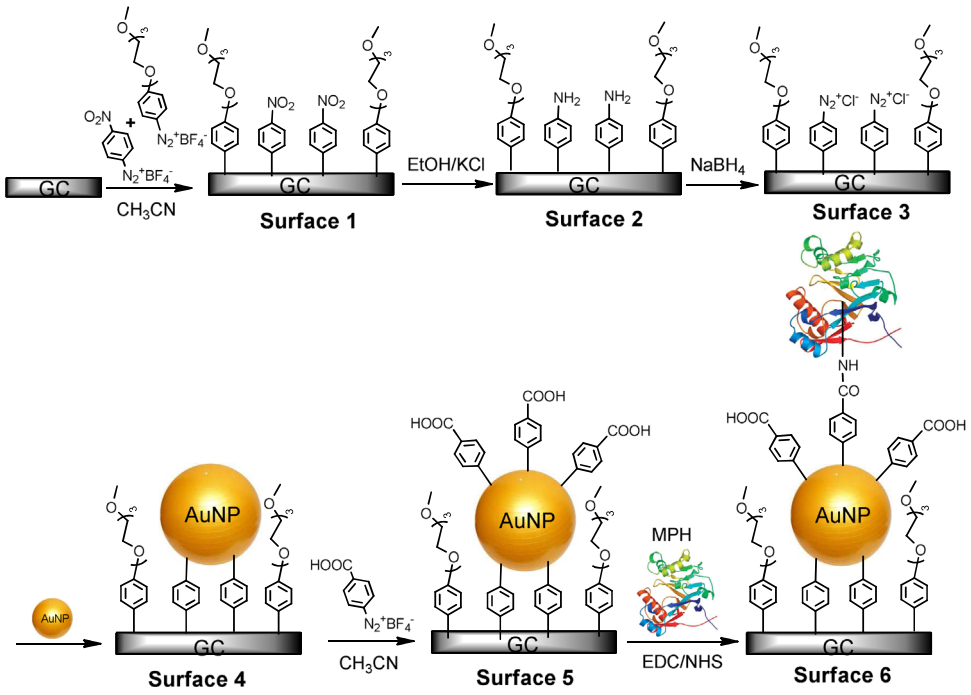

Scheme 1. The scheme for fabrication of sensing interface (surface 6) for detection of methyl parathion.

embedded in epoxy resin (GaossUnion, Wuhan). All experiments utilized a Pt secondary electrode with Ag/AgCl (3.0 M NaCl) reference electrode. All voltammetric measurements were obtained with the scan rate of 100 mV s^{-1}. All CV and square wave voltammetry (SWV) measurements were carried out in pH 7.0 phosphate buffers. X-ray photoelectron spectra (XPS) were collected from GC plates on a VG multilab 2000 spectrometer with a monochromated Al *K*α source (1486.6 eV), hemispherical analyzer and multichannel detector. The spectra were calibrated on the C1s peak (285.0 eV). The quoted percentage coverage for the different elements and sub-groups were estimated from the corresponding fitted areas and associated sensitivity factors. Scanning electron microscopy (SEM) was carried out using a Hitachi S-900 SEM (Berkshire, England).

3. Results and discussions

By forming mixed monolayers, surfaces can be modified with multiple functionalities with something close to molecule level control (Liu et al., 2010; Liu and Gooding, 2006), which is particularly attractive for fabrication of sensing and biosensing interfaces where a specific interaction with a variety of species in solution is required. Thus GC electrodes herein were firstly modified with mixed monolayers of 4-nitrophenyl/PEG (Scheme 1) which is helpful to provide the interface for attaching AuNP and resisting non-specific protein adsorption. Fig. 1a shows the electrochemistry in 0.05 M H_2SO_4 for GC surfaces before and after attachment of AuNPs. The appearance of a reductive peak at about 0.8 V confirms the successfully attachment of AuNPs to the GC interface. In addition, the CV is very stable with 10 cycles. The successful attachment of AuNP with the diameter of about 15 nm to the surface was also confirmed by SEM (Fig. 1b). The number of AuNP in SEM images was counted manually, and the AuNP densities were then calculated from the typical SEM images on GC surfaces.

To maximize the density of AuNPs on interfaces, five approaches for achieving surface 4 were studied: (1) in situ modification of 4-aminophenyl followed by incubation in 0.5 M HCl containing $NaNO_2$ for overnight; (2) in situ modification of 4-aminophenyl followed by incubation in a basic solution (phosphate buffer, pH=10) containing 10 mM $NaBH_4$ for overnight; (3) modification of 4-nitrophenyl followed by converting 4-nitrophenyl to 4-aminophenyl in a protic solution, and then incubation in 0.5 M HCl containing $NaNO_2$ for overnight; (4) modification of 4-nitrophenyl followed by converting 4-nitrophenyl to 4-aminophenyl in a protic solution, and then incubation in a basic solution (phosphate buffer, pH=10) containing 10 mM $NaBH_4$ for overnight. After that, the modified surfaces in above 4 methods were treated with AuNPs solution by fixing potential at −0.4 V for 240 s, respectively; (5) it is the same as approach 4) except the modified surface was treated with AuNPs solution by scanning CV between −0.5 V and 0.5 V for 2 cycles at 100 mV s^{-1}. The density of AuNPs was calculated form SEM images and listed in Fig. S1. Maximum AuNPs density (329×10^{-8} AuNP cm^{-2}) was obtained using the surface aryldiazonium salt modification method 4, which is six times higher than that of AuNPs using method 1 (73×10^{-8} AuNP cm^{-2}). The low density of AuNP on electrode might be due to the formation of multilayers of 4-aminophenyl during the in situ modification and the incomplete conversion of amine groups to diazonium groups. It is also observed that treatment of modified GC surface in AuNP by fixing potential provides higher density than that by scanning CV. As we studied previously adding a potential to the surface can initiate electrochemical attachment of the AuNPs, which happens between −0.1 V and −0.3 V (Liu et al., 2011). Thus fixing a potential at −0.4 V is helpful to completely convert the diazonium to a phenyl radical followed by attachment of AuNPs resulting in the higher AuNPs density.

XPS was used for the characterization of the fabricated sensing interfaces. Fig. S2 shows the N1s core level spectra for bare GC, surface 1–4. No N1s species were observed at bare GC surfaces. Table S1 lists the XPS atomic percentage of different nitrogen

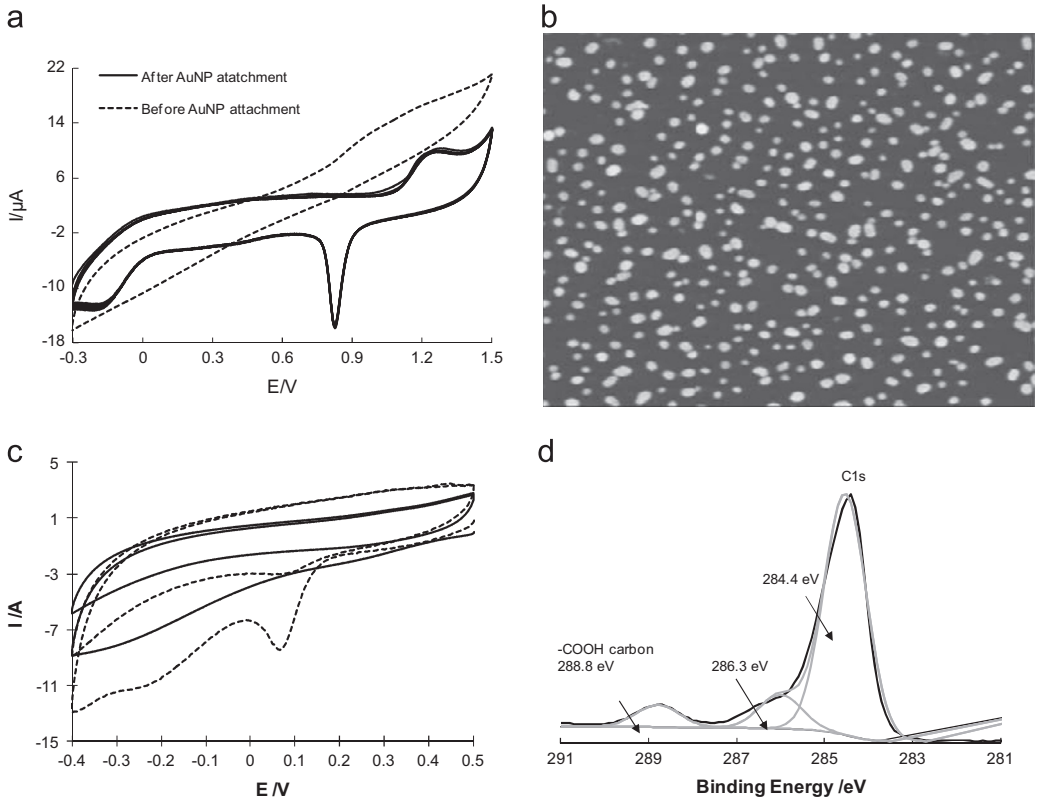

Fig. 1. (a) CV of the GC surfaces before and after the covalent attachment of AuNPs. in 0.05 M H_2SO_4 at the scan rate of 100 mV s^{-1}. (b) SEM images of GC surfaces after the covalent attachment of AuNPs with the magnification of 100 K. (c) CV of modification of surface 3 (solid line) and surface 4 (dotted line) with 4-carboxylphenyl diazonium salts. (d) C1s core level spectra for surface 5. Insert: surface 3 after modification of 4-carboxylphenyl species.

species on different modified surfaces. For surface 1, the peaks at around 406 eV were observed and assigned to the nitrogen of the nitro group of the 4-nitrophenyl layers. The observation of nitrogen signal at around 400 eV present in 4-nitrophenyl film derived from diazonium salt reductive deposition is consistent with previous reports, which suggested this 400 eV nitrogen peak arises from nitrogen atoms in azo groups (Ph–N=N–Ph), formed when a multilayer develops. The percentage of azo groups is estimated to be 12% in the N1s XPS peak, which is consistent with that observed by Lyskawa and Belanger (2006) After the electrochemical reduction of the nitro group, the N1s narrow scan spectra peaks at 406.3 eV and 400.2 eV still exist with the peak at 406.3 eV showing a significant decrease in intensity but the peak at 400.2 eV showing an appreciate increase in intensity. The increase of N1s peak at 400.2 eV for surface 2 was reasonably assigned to the nitrogen of amine groups resulting from the reduction of 4-nitrophenyl. The percentage of N1s at 406.3 eV is estimated to be 5% of the total nitrogen species in surface 2, suggesting around 95% nitro groups have been reduced to amino groups. For surface 3, the peaks at 403.7 and 405.6 eV are characteristic of diazonium groups (Combellas et al., 2005; Finn and Jolly, 1972; Lyskawa and Belanger, 2006) and thus demonstrates that the amino groups have been converted to diazonium moieties during the chemical treatment at $NaBH_4$ aqueous solution for overnight. The component at the higher binding energy (405.6 eV) is due to the N closest to the phenyl ring. The total percentage of N species decreased from 10.9% at surface 3 to 1.3% at surface 4 (Table S1). Considering the presence of 12% of azo groups, it is estimated that almost 100% of the amine groups have been converted to diazonium moieties under this conditions. This result suggests that applying a negative potential to surface 4 converted the diazonium moieties to radicals with the loss of N_2, and the attachment of the AuNP is assumed to be via stable C–Au bonds (Liu et al., 2007).

CV of modification of surface 4 with 4-carboxylphenyl was shown in Fig. 1c. A reductive peak centred at around 0.09 V was observed at the first scan suggesting the successful attachment of 4-carboxylphenyl species to AuNP, which was further confirmed by C1s core level spectra for surface 5 (Fig. 1d). The appearance of C1s peak at 288.8 eV indicates the presence of carbolic acid groups on surface 5. For this modification step we aim to fabricate the 4-carboxylphenyl groups to AuNP surfaces to maximize the function of AuNP as electronic bridges on sensing interface, but it might be possible for 4-carboxylphenyl groups to be modified to GC surfaces. In order to clarify the exact location of carboxylic acid groups, one control was carried out by modification of surface 3 (before the attachment of AuNP) with 4-carboxylphenyl. The absence of the reductive peak in the CV (Fig. 1c solid line) might indicate that 4-carboxylphenyl species cannot be modified to surface 3 which has been already modified with phenyl groups and PEG. The C1s peak at 288.8 eV was not observed after modification of surface 3 with 4-carboxylphenyl (Fig. 1d insert). This control suggests that 4-carboxylphenyl species were modified to the AuNP surfaces but not the GC surfaces.

CV was employed to investigate the electrochemistry of various modified GC electrodes in $Fe(CN)_6^{3-}/Fe(CN)_6^{4-}$ redox couple solution. Fig. S3 shows the cyclic voltammograms of bare GC electrode, and the stepwise attachment of 4-nitrophenyl, AuNP, and MPH on GC surfaces. The well-defined peak characteristic of $Fe(CN)_6^{3-}/Fe(CN)_6^{4-}$ was observed on bare GC electrodes. However, the 4-nitrophenyl surface resulted in prevention of access of the $Fe(CN)_6^{3-}/Fe(CN)_6^{4-}$ redox species to the electrode and hence no Faradaic peaks for ferricyanide were observed between -0.2 V to $+0.6$ V. An increase in the peak current of the redox couple was observed (Fig. S3 dash dotted line) after the attachment of AuNP. This increase in electron transfer rate upon attachment of AuNPs is consistent with previous observations which shows that the

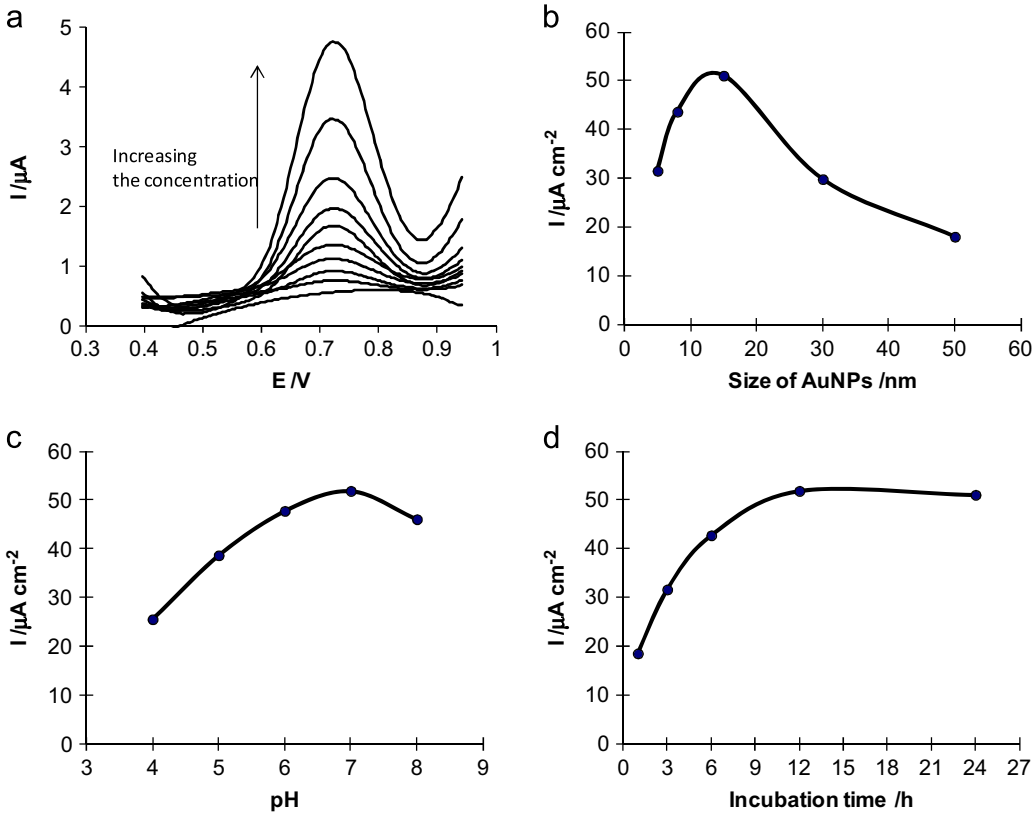

Fig. 2. (a) SWV curves for the sensing interface after incubation in methyl parathion solutions with the concentrations of 0, 0.2, 0.3, 0.4, 0.5, 1, 2, 3, 10 and 50 ppb, respectively, and the effect of (b) size of AuNPs, (c) pH of phosphate buffer, and (d) incubation time of MPH on the response of the fabricated biosensor to 10 ppb methyl parathion.

nanoparticles can increase the electronic coupling to the underlying electrode (Chen et al., 1998; Shein et al., 2009). After modification of 4-carboxylphenyl species on AuNP surfaces, the peak current of the redox couple decreased, showing surface 5 restricted the access of $Fe(CN)_6^{3-}/Fe(CN)_6^{4-}$ redox probe to the AuNP surface due to the presence of 4-carboxylphenyl groups. With the further immobilization of MPH, the peak current of redox couple decreased significantly (Fig. S3 solid line), which indicates MPH has been successfully attached on the surfaces of AuNP; thus covering AuNPs with protein and inhibiting access of the $Fe(CN)_6^{3-}/Fe(CN)_6^{4-}$ redox couple to the electroactive elements on the surface.

The herein biosensor principle is based on the methyl parapthion catalysis by MPH to produce *p*-nitrophenol, which is electroactive and can be oxidized to generate measurable current which is related to the concentration of methyl parathion. Fig. 2a shows SWV of the sensing interface after incubation in methyl parathion solutions with different concentrations. A significant peak at around 0.71 V corresponding to oxidation of *p*-nitrophenol was observed and increased with the concentration of methyl parathion. However, no peak was observed when AuNP was omitted in the fabrication steps, which indicates AuNPs function as electronic bridges between MPH and electrodes. To maximize the sensitivity of the fabricated biosensor, the effect of size of AuNPs, pH and incubation time of MPH on detection of methyl parathion were investigated. With the diameter increase from 5 nm to 50 nm, the sensing interface produced a bell-shaped response curve (Fig. 2b). The maximum electrochemical response was obtained at the size of 15 nm. The peak potential for methyl parathion shifted negatively with increasing pH from 4.0 to 7.0 (Fig. 2c), while the highest peak current was obtained at pH = 7.0. The electrochemical signal increased with incubation time of MPH and stabilized after 12 h (Fig. 2d), indicating maximum surface coverage of MPH was obtained after incubation of 12 h.

The specificity of fabricated sensing interface against other organophosphorus pesticides such as paraoxon, parathion, malathion, monocrotophos, dimethoate, and dietheyl phosphate was investigated (Fig. 3a). There was no obvious current change after incubation with other organophosphorus pesticides except parathion which showed an ignorable current. It indicates that the fabricated sensing interface has the highest specificity for methyl parathion, and no affinity to other members of the organophosphorus pesticides in the interested concentration range. The high specificity of fabricated sensing interface might be due to the presence of PEG which has the ability to resist the non specific protein adsorption (Liu and Gooding, 2006), and the high hydrolytic affinity of MPH to methyl parathion. The calibration curve (Fig. 3b) shows the current density versus the logarithm of the concentration of methyl parathion in 0.05 M phosphate buffer (0.05 M KCl, pH 7.0). The linear concentration range was from 0.2 ppb to 100 ppb. The linear regression equation, $I\ (\mu A\ cm^{-2}) = 22.815 \log_{10} C^{(ppb)} + 25.505$ with the correlation coefficient of 0.9922 can be obtained. The detection limit for methyl parathion is 0.07 ppb ($S/N = 3$), which is lower than that in the literature (0.1 ppb) (Zhao et al., 2013).

Under optimal experimental conditions, the fabricated sensing interface provided similar electrochemical signal after ten repeated measurements with a relative standard deviation of 2.23% (Fig. 4a), indicating the fabricated sensing interface is very stable and not poisoned by methyl parathion. Based on weekly usage, the sensing interface remained over 90% of activity after 10 weeks storage at a phosphate buffer solution at 4 °C (Fig. 4b). It suggests the fabricated sensing interface is very stable, which is

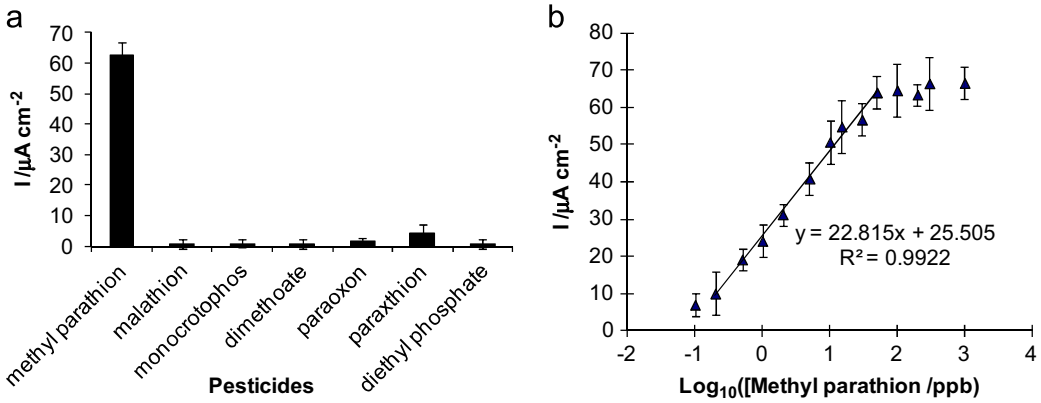

Fig. 3. (a) The current density at 0.71 V after incubation of surface 6 with the corresponding pesticides at the concentration of 50 ppb. (b) A calibration curve showing the current density with the logarithm of the concentration of methyl parathion in 0.05 M phosphate buffer (0.05 M KCl, pH 7.0). Error bars are ±1 standard deviation of the current densities of four different electrodes.

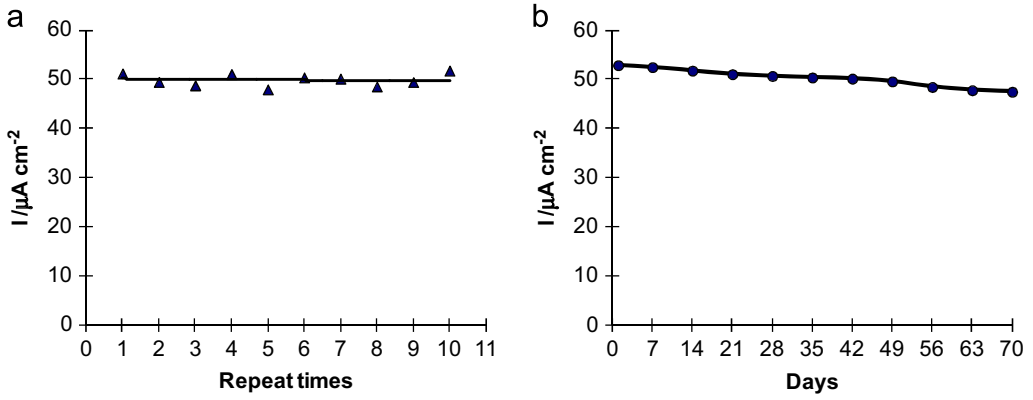

Fig. 4. (a) The continuous use stability and (b) the shelf-life stability studies of the fabrication biosensor for detection of 10 ppb methyl parathion.

Table 1
Comparison of analytical performance of the proposed biosensor with other published sensors based on organophosphorus hydrolase (OPH).

Sensors	pH	Linear range	Detection limit	Stability	Reproducibility (RSD)	Reference
MPH Colorimetric assay	7.5	–	1 mg L^{-1}	3 Months	< 10%	Anh et al. (2011)
MPH/SP@AuNPs/MWNTs	7	0.001–5.0 μg mL^{-1}	0.3 ng mL^{-1}	30 Days	2.10%	Chen et al. (2011)
MPH/F_3O_4@Au nanocomposites	7.4	0.5–1000 ng mL^{-1}	0.2 ng mL^{-1}	30 Days	7.80%	Zhao et al. (2013)
MPDE/QD/Cys/Au_{nano}/MWNTs	7.4	5.0–200 ng mL^{-1}	1.0 ng mL^{-1}	30 Days	8.70%	Du et al. (2010)
OPH_{6His}/Fluorescence assay	8.5	10–500 ng mL^{-1}	~50 ng mL^{-1}	–	1.51%	Thakur et al. (2012)
OPH/CNT biosensor	7.4	2–10 μM	0.8 μM	–	–	Deo et al. (2005)
MPH/AuNP biosensor	7	0.2–100 ng mL^{-1}	0.07 ng mL^{-1}	10 Weeks	4.28%	This work

"–" Means the data was not reported.

consistent with the high stability of AuNP modified surface by Au–C bonding (Liu et al., 2011). The reproducibility was evaluated by testing the current responses of six separately prepared sensing interfaces for 10 ppb methyl parathion with the relative standard deviation of 4.28%. The recoveries obtained for six real samples, which were spiked with 20 ppb methyl parathion, ranged from 93 to 107% based on the average of three separate measurements (Table S2). The satisfied recoveries were also obtained for soil (96%) and green tea sample (93%), indicating the solubility of methyl parathion in aqueous solution is appreciable in ppb level. The comparison of analytical performance of the herein biosensor with other published methyl parathion sensors is shown in Table 1. The results reveal that the MPH/AuNP biosensor herein has comparative advantages in lowest detection limit, reproducibility, and stability although the linearity range is slightly compromised.

4. Conclusions

Herein, tethering AuNPs to GC surfaces using surface bound diazonium salts was investigated as a strategy to produce stable AuNP surfaces for fabricating a biosensor of methyl parathion. GC electrodes were first modified with mixed monolayers of 4-nitrophenyl/PEG followed by converting nitro groups to amine groups, and then the terminal amine groups were converted to diazonium groups in the presence of $NaBH_4$ to form surface 3. Subsequently AuNP were immobilized on the interface by electrochemical reduction at −0.4 V for 240 s to achieve a 4-phenyl AuNP modified interface (surface 4). Then 4-carboxylphenyl species were introduced to AuNP surface followed by covalent atatchment of MPH to achieve surface 6. The fabricated biosenser shows high sensitivity, specificity, reproducibility and stability to methyl

parathion, and can be used for detection of methyl parathion in phosphate buffer solution in the range of 0.2 ppb and 100 ppb with the detection limit of 0.07 ppb. The satisfied recoveries were obtained for detection of methyl parathion spiked in real samples. This AuNP fabricated interface is potential for fabrication of other stable biosensors for on-site detection of a spetrum of pesticides in real samples.

Acknowledgements

This work was financially supported by the National Natural Science Foundation of China (Grant 209237057) and the self-determined research funds of CCNU from the colleges' basic research and operation of MOE (2020513000613).

Appendix A. Supplementary material

Supplementary data associated with this article can be found in the online version at http://dx.doi.org/10.1016/j.bios.2013.10.025.

References

Anh, D.H., Cheunrungsikul, K., Wichitwechkarn, J., Surareungchai, W., 2011. Biotechnol. J. 6, 565–571.
Chen, S., Murray, R.W., Feldberg, S.W., 1998. J. Phys. Chem. B 102, 9898–9907.
Chen, S.Z., Huang, J., Du, D., Li, J.L., Tu, H.Y., Liu, D.L., Zhang, A.D., 2011. Biosens. Bioelectron. 26, 4320–4325.
Chough, S.H., Mulchandani, A., Mulchandani, P., Chen, W., Wang, J., Rogers, K.R., 2002. Electroanalysis 14, 273.
Combellas, C., Delamar, M., Kanoufi, F., Pinson, J., Podvorica, F.I., 2005. Chem. Mater. 17, 3968–3975.
Deo, R.P., Wang, J., Block, I., Mulchandani, A., Joshi, K.A., Trojanowicz, M., Scholz, F., Chen, W., Lin, Y., 2005. Anal. Chim. Acta 530, 185–189.
Dong, Y., Bartlam, M., Sun, L., Zhou, Y., Zhang, Z., Zhang, C., Rao, Z., Zhang, X., 2005. J. Mol. Biol. 353, 655–663.
Du, D., Chen, W., Zhang, W., Liu, D., Li, H., Lin, Y., 2010. Biosens. Bioelectron. 25, 1370–1375.
Finn, P., Jolly, W.L., 1972. Inorg. Chem. 11, 1434–1435.
Frens, G., 1973. Nature 241, 20–22.
Gaberlein, S., Knoll, M., Spener, F., Zaborosch, C., 2000. Analyst 125, 2274.
Gao, X., Tang, G., Su, X., 2012. Biosens. Bioelectron. 36, 75–80.
Giordano, B.C., Collins, A.G.E., 2007. Curr. Org. Chem. 11, 255–256.
Gong, J.M., Wang, L.Y., Song, D.D., Zhu, X.L., Zhang, L.Z., 2009. Biosens. Bioelectron. 25, 493–496.
Gooding, J.J., 2008. Electroanalysis 20, 573–582.
GutiéRrez-SáNchez, C., Pita, M., Vaz-Domínguez, C., Shleev, S., De Lacey, A.L., 2012. J. Am. Chem. Soc. 134, 17212–17220.
Katz, E., Willner, I., Wang, J., 2004. Electroanalysis 16, 19–44.
Leandro, C.C., Hancock, P., Fussell, R.J., Keely, B.J., 2007. J. Chromatogr., A 1166, 152–162.
Liu, G.Z., Bocking, T., Gooding, J.J., 2007. J. Electroanal. Chem. 600, 335–344.
Liu, G.Z., Chockalingham, M., Khor, S.M., Gui, A.L., Gooding, J.J., 2010. Electroanalysis 22, 918–926.
Liu, G.Z., Gooding, J.J., 2006. Langmuir 22, 7421–7430.
Liu, G.Z., Iyengar, S.G., Gooding, J.J., 2012. Electroanalysis 24, 1509–1516.
Liu, G.Z., Liu, J.Q., Bocking, T., Eggers, P.K., Gooding, J.J., 2005. Chem. Phys. 319, 136–146.
Liu, G.Z., Luais, E., Gooding, J.J., 2011. Langmuir 27, 4176–4183.
Lyskawa, J., Belanger, D., 2006. Chem. Mater. 18, 4755–4763.
Mercey, G., Verdelet, T., Renou, J., Kliachyna, M., Baati, R., Nachon, F., Jean, L., Renard, P.Y., 2012. Acc. Chem. Res. 45, 756–766.
Oliveiraa, J.E., Scagiona, V.P., Grassia, V., Correaa, D.S., Mattosoa, L.H.C., 2012. Sens. Actuators, B 171-172, 249–255.
Sacks, V., Eshkenazi, I., Neufeld, T., Dosoretz, C., Rishpon, J., 2000. Anal. Chem. 72, 2055–2061.
Sharmaa, S.P., Tomara, L.N.S., Acharyaa, J., Chaturvedia, A., Suryanarayana, M.V.S., Jain, R., 2012. Sens. Actuators, B 166-167, 616–623.
Shein, J.B., Lai, L.M.H., Eggers, P.K., Paddon-Row, M.N., Gooding, J.J., 2009. Langmuir 25, 11121–11128.
Sun, L., Dong, Y., Zhou, Y., Yang, M., Rao, Z., Zhang, X.E., 2004. Acta Crystallogr. D 60, 954–956.
Thakur, S., Reddy, M.V., Siddavattam, D., Paul, A.K., 2012. Sens. Actuators, B 163, 153–158.
Zhao, J.J., Bradbury, C.R., Huclova, S., Potapova, I., Carrara, M., Fermín, D.J., 2005. J. Phys. Chem. B 109, 22985–22994.
Zhao, Y., Zhang, W., Lin, Y., Du, D., 2013. Nanoscale 5, 1121–1126.